Supporting Information for "ISources of uncertainty in regional and global terrestrial CO_2-exchange estimates"

A. Bastos[1], M. O'Sullivan[2], P. Ciais[3], D. Makowski[4,5], S. Sitch[2], P. Friedlingstein[6], F. Chevallier[3], C. Rödenbeck[7], J. Pongratz[1,87], I. T. Luijkx[9], P.K. Patra[10], P. Peylin[3], J.G. Canadell[11], R. Lauerwald[12], W. Li[13], N. E. Smith[9], W. Peters[9,14], D.S. Goll[15], A.K. Jain[16], E. Kato[17], S. Lienert[18], D.L. Lombardozzi[19], V. Haverd[20], J.E.M.S. Nabel[8], B. Poulter [21], H. Tian[22], A.P. Walker[23], S. Zaehle[7]

[1]Ludwig-Maximilians Universität, Deptartment of Geography, Luisenstr. 37, 80333, München, Germany

[2]College of Life and Environmental Sciences, University of Exeter, Exeter EX4 4RJ, UK

[3]Laboratoire des Sciences du Climat et de l'Environnement (LSCE), CEA-CNRS-UVSQ, UMR8212, 91191 Gif-sur-Yvette, France

[4]University Paris-Saclay, AgroParisTech, INRAE, UMR 211, 78850 Thiverval-Grignon France

[5]CIRED 45bis Avenue de la Belle Gabrielle, 94130 Nogent-sur-Marne France

[6]College of Engineering, Mathematics and Physical Sciences, University of Exeter, Exeter EX4 4QF, UK

[7]Max Planck Institute for Biogeochemistry, 07745 Jena, Germany

[8]Max Planck Institute for Meteorology, 20146 Hamburg, Germany

[9]Department of Meteorology and Air Quality, Wageningen University & Research, P.O. Box 47, 6700AA Wageningen, the Netherlands.

[10]Research Institute for Global Change, Japan Agency for Marine-Earth Science and Technology (JAMSTEC), Yokohama, Japan

[11]CSIRO Oceans and Atmosphere, Canberra, 2601, Australia

[12]Dept. Geoscience, Environment & Society (DGES), CP160/02 Université Libre de Bruxelles 50, av. F.D. Roosevelt, 1050 Bruxelles, Belgium

[13]Ministry of Education Key Laboratory for Earth System Modeling, Department of Earth System Science, Tsinghua University, Beijing, China

[14]Centre for Isotope Research, University of Groningen, Nijenborgh 6, 9747 AG Groningen, the Netherlands.

[15]Department of Geography, University of Augsburg, Augsburg, Germany

[16]Department of Atmospheric Sciences, University of Illinois, Urbana, IL 61801, USA

[17]Institute of Applied Energy (IAE), Minato, Tokyo 105-0003, Japan

[18]Climate and Environmental Physics, Physics Institute and Oeschger Centre for Climate Change Research, University of Bern, Bern CH-3012, Switzerland

[19]Climate and Global Dynamics Laboratory, National Center for Atmospheric Research, Boulder, CO 80302, USA

[20]CNRM, Universit de Toulouse, Mto-France, CNRS, Toulouse, France

[21]NASA, Biospheric Sciences Lab, Greenbelt, MD, USA

[22]International Center for Climate and Global Change Research, School of Forestry and Wildlife Sciences, Auburn University, 602 Duncan Drive, Auburn, AL 36849, USA

[23]Environmental Sciences Division and Climate Change Science Institute, Oak Ridge National Laboratory, Oak Ridge, TN, 37831, USA

Contents of this file

References

FAO. (2015). *Global forest resources assessment 2015 (fra2015)* (Tech. Rep.). Rome: Food and Agriculture Organization of the United Nations.

FAOSTAT. (2015). Faostat: Food and agriculture organization of the united nations.. Retrieved from http://www.fao.org

Hurtt, G., Chini, L., Sahajpal, R., Frolking, S., Bodirsky, B. L., Calvin, K., ... Zhang, X. (2017). *Harmonization of global land use scenarios (luh2): Historical v2.1h.* Earth System Grid Federation. Retrieved from https://doi.org/10.22033/ESGF/input4MIPs.1127

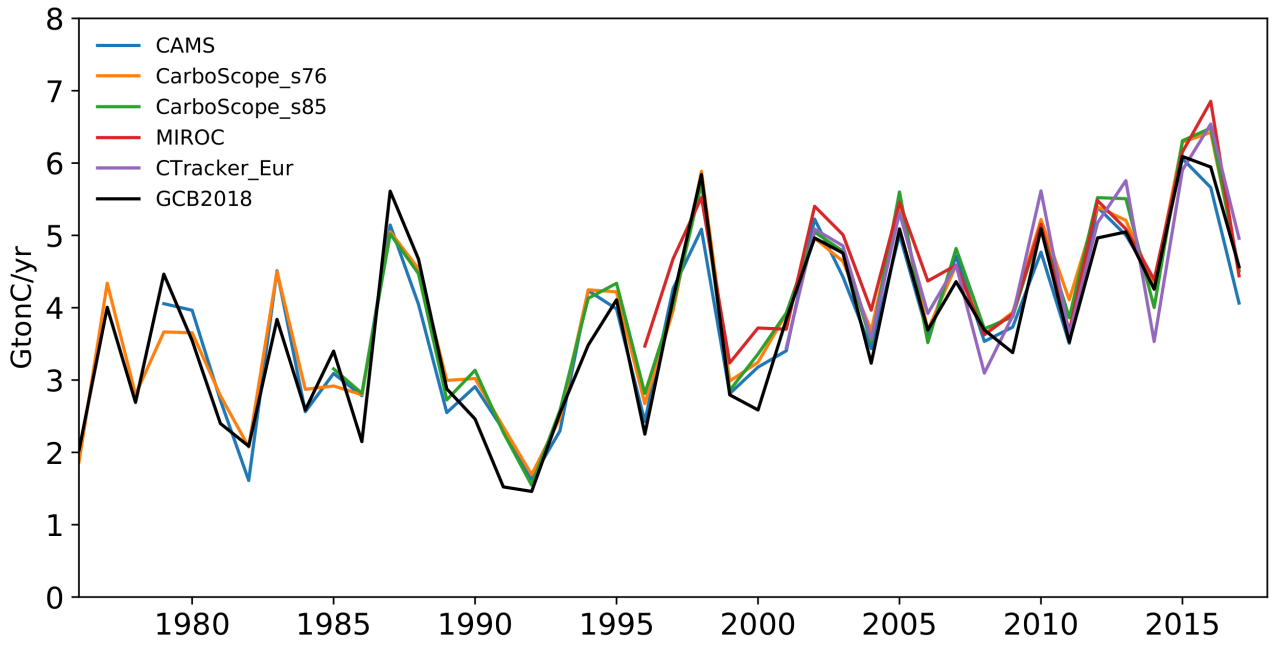

Figure S1. Comparison of atmospheric CO_2 growth-rate (G_{ATM}) from GCB2018 (black) and from each of the five inversions used in this study.

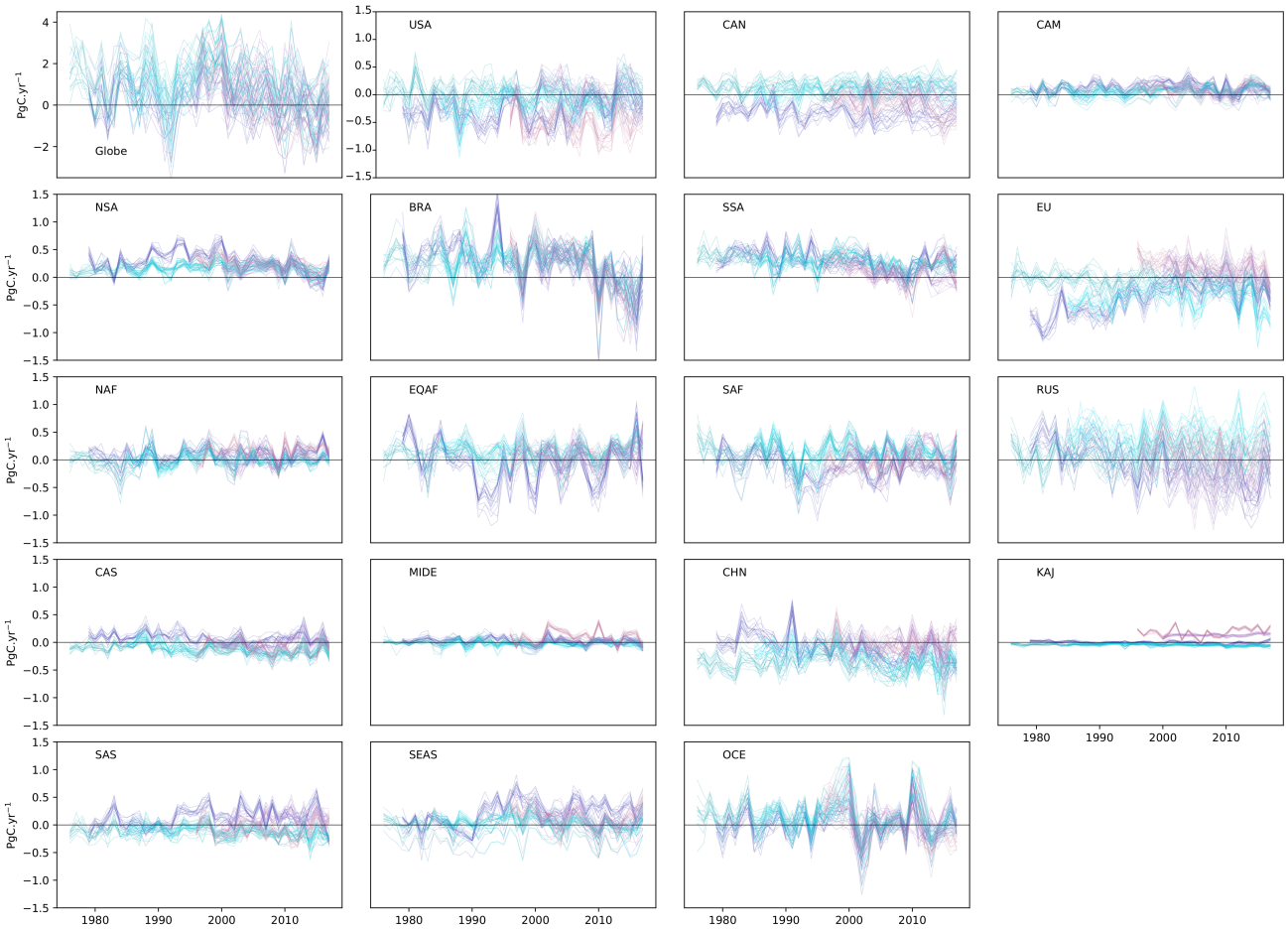

Figure S2. Regional estimates of D for the 5 inversions $\times$ 16 DGVMs ensemble. Each color indicates one inversion as in Fig. 1.

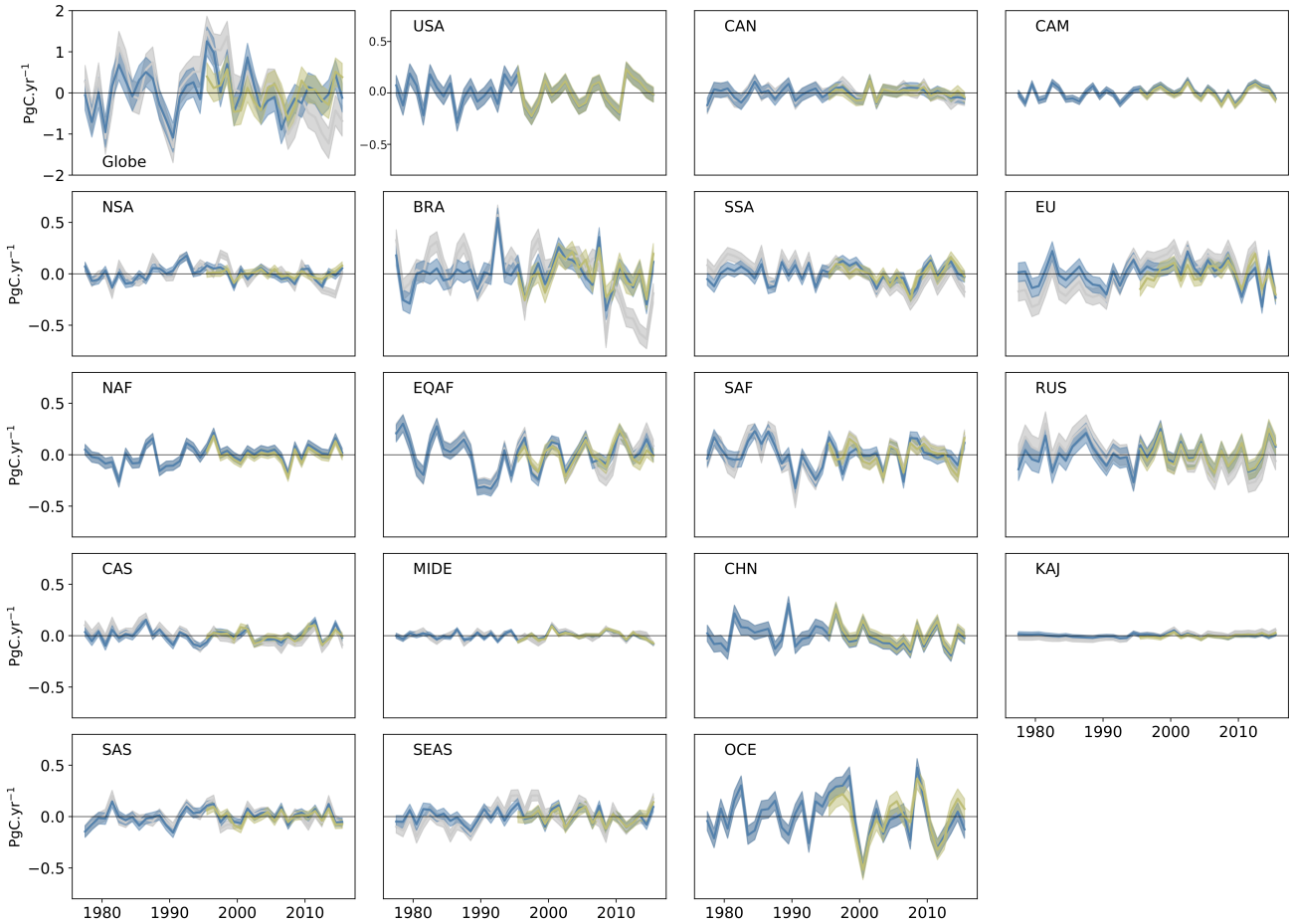

Figure S3. Residuals of the different LME fits: $\mathrm{LME_{RE}}$ between 1979-2017 in grey, $\mathrm{LME_{FE}}$ without fire between 1979-2017 in blue and $\mathrm{LME_{FE}}$ with fire, fit for 1997-2017 in yellow.

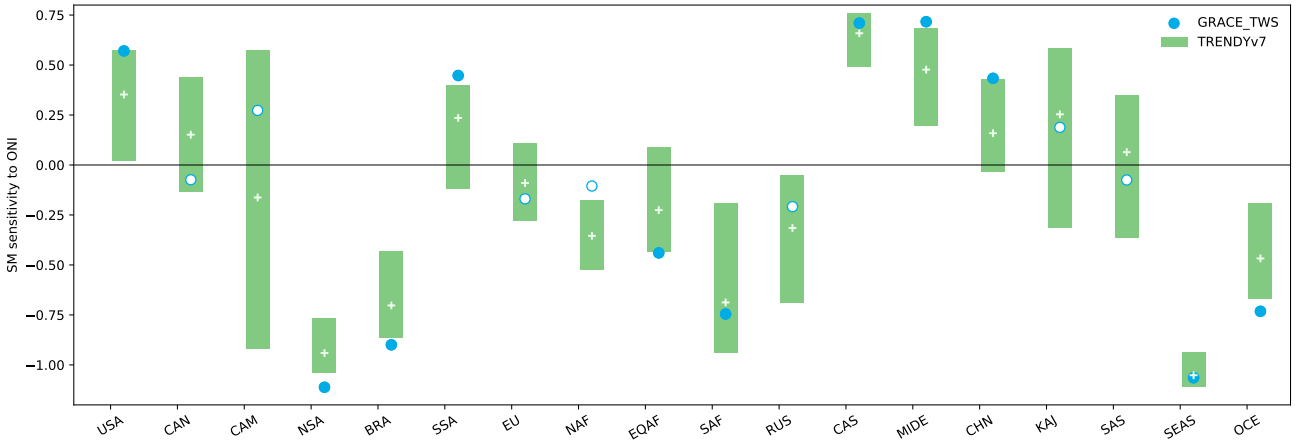

Figure S4. Sensitivity of total water storage from GRACE total water storage (TWS) reconstruction to ONI (blue circles) and the sensitivity of simulated soil moisture from DGVMs to ONI. For comparability with Fig. 5, the time-series of both total water storage and simulated soil-moisture have been normalised. The full circles indicate those regions where the sensitivity of TWS to ONI is significant ($p - value < 0.05$), and the open circles indicate non-significant values.

According to Fig. 4, ONI has significant effects on D in NSA, BRA, SAF and SEAS (negative) and CAS, MIDE and SAS (positive). In NSA, BRA, SEAS, and CAS the DGVM spread is small and the DGVM ensemble mean (MMEM) is close to the value of the sensitivity of TWS to ONI. In SAF, the MME is close to the TWS-ONI sensitivity value, but the DGVMs show large spread in their estimates. In MIDE, DGVMs underestimate the sensitivity of soil water to ONI and how a wide range, but GRACE TWS does not show a significant relationship. Both GRACE TWS and MMEM SM show a non-significant sensitivity of water-availability to ONI in SAS.

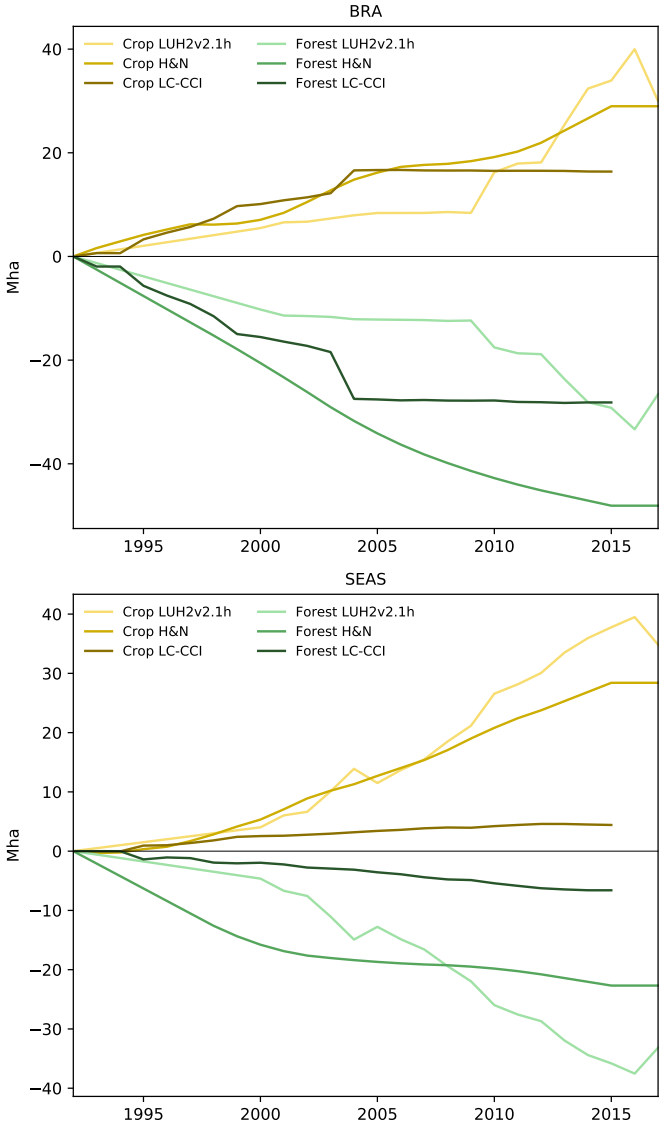

Figure S5. Changes in cropland and forest extent between 1979 and 2015/2017 from HN2017 (adapted from (FAO, 2015; FAOSTAT, 2015)), LUH2v2.1h (Hurtt et al., 2017) and ESA-CCI Land-Cover .

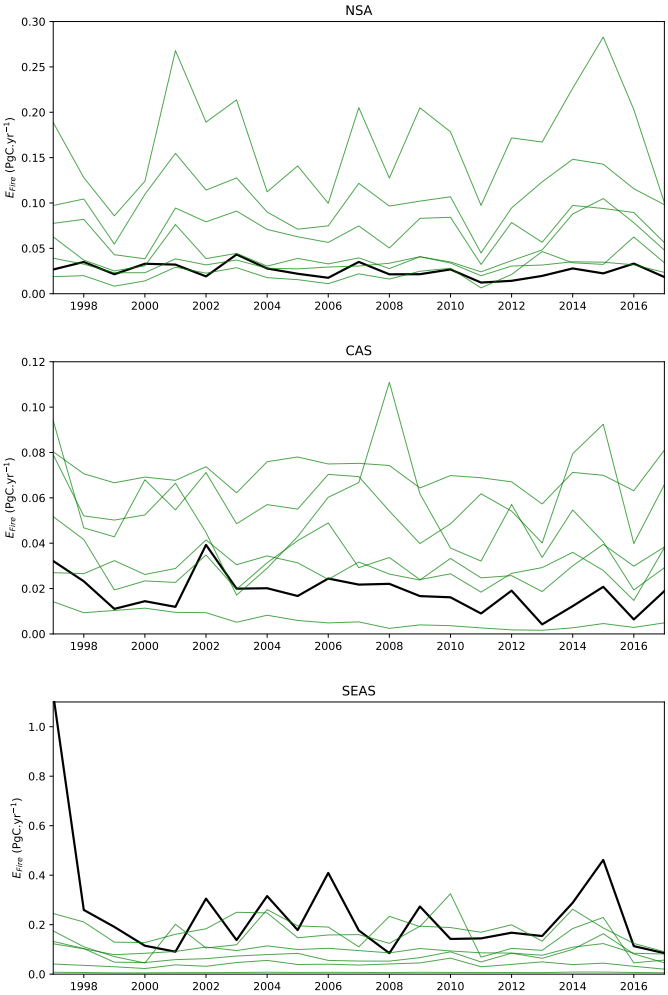

Figure S6. Temporal variability of E_{fire} from GFED4.1s (black lines) and simulated by DGVMs (green lines) for the three regions where fires have significant effects in D.

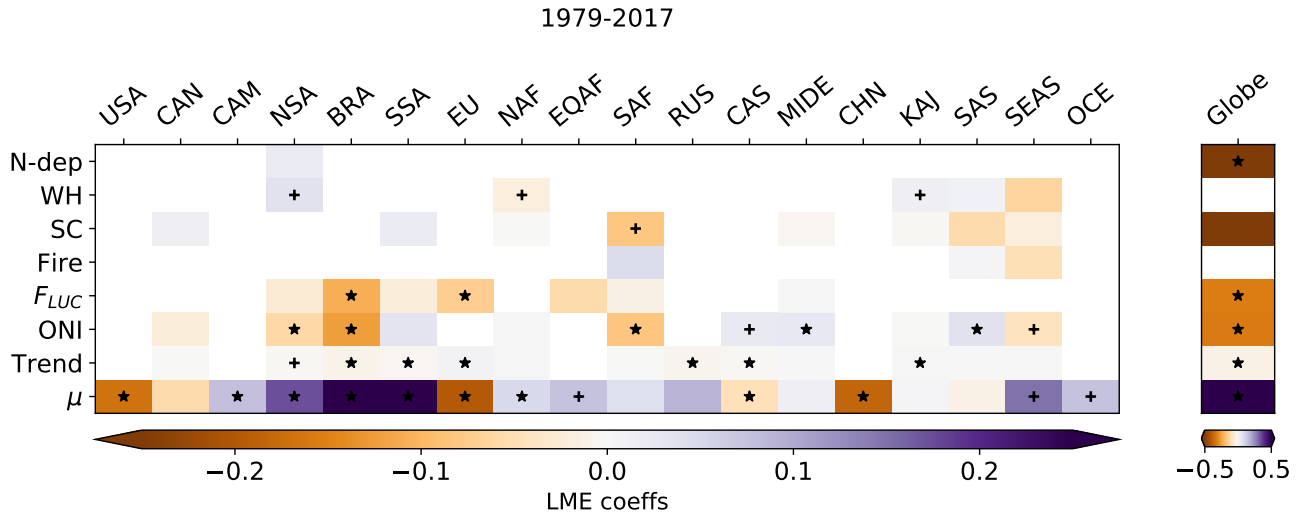

Figure S7. Coefficients of the LME model fit with fixed effects including, in addition to those in Fig. 4, the processes included or not in DGVMs (Table 1): fire, shifting cultivation (SC), wood-harvest (WH) and N-deposition (N-dep).

Table S1. Regional and global bias (μ) estimated for the LME fit to different subsets of DGVMs, compared to the full ensemble. The asterisks indicate those values where the bias for the model sub-set is significantly different from that of the full ensemble, given its uncertainty.

Region	All DGVMs	Fire only	SC only	WH only	N-dep. only
USA	-0.17±0.03	-0.16	-0.15	-0.15	-0.17
CAN	-0.05±0.02	-0.05	-0.04	-0.04	-0.05
CAM	0.08±0.02	0.08	0.06	0.07	0.08
NSA	0.21±0.01	0.21	0.22	0.22	0.21
BRA	0.26±0.04	0.29	0.25	0.26	0.26
SSA	0.26±0.02	0.26	0.27	0.27	0.26
EU	-0.20±0.03	-0.20	-0.20	-0.19	-0.20
NAF	0.04±0.02	0.04	0.03	0.03	0.04
EQAF	0.07±0.03	0.06	0.03*	0.05	0.07
SAF	0.03±0.03	0.04	0.00	0.02	0.03
RUS	0.09±0.05	0.07	0.09	0.11	0.09
CAS	-0.05±0.01	-0.05	-0.05	-0.04	-0.05
MIDE	0.013±0.007	0.016	0.011	0.011	0.013
CHN	-0.18±0.02	-0.18	-0.19	-0.18	-0.18
KAJ	0.013±0.004	0.014	0.019*	0.019*	0.014
SAS	-0.02±0.02	-0.03	-0.05*	-0.03	-0.02
SEAS	0.07±0.03	0.05	0.02*	0.05	0.07
OCE	0.08±0.04	0.08	0.07	0.08	0.08
Globe	0.68±0.18	0.62	0.45*	0.66	0.68